Dynein light chain-dependent dimerization of Egalitarian is essential for maintaining oocyte fate in *Drosophila*.

Hannah Neiswender[1], Chandler H. Goldman[1, 2], Rajalakshmi Veeranan-Karmegam[1], Graydon B. Gonsalvez[1*]

[1]Cellular Biology and Anatomy,
Medical College of Georgia, Augusta University
1460 Laney Walker Blvd,
Augusta, GA, 30912, USA

[2]Present address
University of Georgia
Department of Genetics
Davidson Life Sciences Complex
120 E. Green St., Athens, GA 30602

Keywords: RNA localization, molecular motor, RNA binding domain, cell polarity, cargo adaptor.

*Address correspondence to
Graydon Gonsalvez (ggonsalvez@augusta.edu)
Cellular Biology and Anatomy
Medical College of Georgia, Augusta University
1460 Laney Walker Blvd. CB2917
Augusta, GA 30912, USA
Tel: (706) 721-1756

ABSTRACT

Egalitarian (Egl) is an RNA adaptor for the Dynein motor and is thought to link numerous, perhaps hundreds, of mRNAs with Dynein. Dynein, in turn, is responsible for the transport and localization of these mRNAs. Studies have shown that efficient mRNA binding by Egl requires the protein to dimerize. We recently demonstrated that Dynein light chain (Dlc) is responsible for facilitating the dimerization of Egl. Mutations in Egl that fail to interact with Dlc do not dimerize, and as such, are defective for mRNA binding. Consequently, this mutant does not efficiently associate with BicaudalD (BicD), the factor responsible for linking the Egl/mRNA complex with Dynein. In this report, we tested whether artificially dimerizing this Dlc-binding mutant using a leucine zipper would restore mRNA binding and rescue mutant phenotypes in vivo. Interestingly, we found that although artificial dimerization of Egl restored BicD binding, it only partially restored mRNA binding. As a result, Egl-dependent phenotypes, such as oocyte specification and mRNA localization, were only partially rescued. We hypothesize that Dlc-mediated dimerization of Egl results in a three-dimensional conformation of the Egl dimer that is best suited for mRNA binding. Although the leucine zipper restores Egl dimerization, it likely does not enable Egl to assemble into the conformation required for maximal mRNA binding activity.

INTRODUCTION

Numerous mRNAs are specifically localized within the cytoplasm of *Drosophila* oocytes and embryos (Suter, 2018). In fact, establishment of oocyte fate, formation of Anterior-Posterior and Dorsal-Ventral polarity, and development of the embryo, all rely on correct localization of specific mRNAs (Weil, 2014). Although several mechanisms can contribute to the localization of mRNA, in many instance, localization requires the minus-end directed microtubule motor, cytoplasmic Dynein (hereafter Dynein) (Goldman and Gonsalvez, 2017). The primary RNA binding protein tasked with linking these diverse transcripts with Dynein is Egalitarian (Egl) (Dienstbier et al., 2009).

Dienstbier and colleagues demonstrated several years back that Egl is able to specifically interact with localization elements found in numerous Dynein-localized cargoes (Dienstbier et al., 2009). In addition to binding RNA, Egl also interacts with BicaudalD (BicD) and Dynein light chain (Dlc/Lc8) (Mach and Lehmann, 1997; Navarro et al., 2004). BicD is a highly conserved adaptor of Dynein and directly interacts with components of the Dynein motor and also with Dynactin, a regulator of Dynein activity (Hoogenraad and Akhmanova, 2016). Dlc is a core component of the Dynein motor, but also appears to have Dynein-independent function. Most notably, recent studies indicate that Dlc can aid in the dimerization of proteins, particularly those such as Egl which harbor long stretches of disordered regions (Barbar, 2008; Rapali et al., 2011; Reardon et al., 2020).

How does Egl link cargo with Dynein? Answering this questions has been the focus of several recent studies. The labs of Simon Bullock and Kathleen Trybus elegantly demonstrated that once Egl binds to cargo, its interaction with BicD is greatly enhanced. This cargo bound complex then associates with Dynein and is required for fully activating Dynein-mediated transport (McClintock et al., 2018; Sladewski et al., 2018). Our lab recently determined that Dlc is required for Egl dimerization (Goldman et al., 2019). Mutations in Egl that compromised Dlc binding were defective for dimerization. These mutants also displayed reduced RNA binding activity, and as a consequence, BicD binding was reduced (Goldman et al., 2019).

The current model in the field is that Egl dimerizes with the aid of Dlc. Dimeric Egl is then able to associate with mRNA cargo. This complex now has a high affinity for BicD, which in turn tethers the entire assemblage onto Dynein for processive minus-end microtubule transport. In support of this model, we showed that artificially dimerizing a mutant version of Egl that could not associate with Dlc was sufficient to restore its ability to bind to mRNA and BicD. These experiments were conducted using lysates from *Drosophila* S2 cells (Goldman et al., 2019). An important question raised by this finding is whether artificially dimerizing Egl could rescue mutant phenotypes in vivo. Answering this question is the focus of the present study. Our results indicate that artificially dimerizing Egl does in fact restores BicD binding. However, in vivo, mRNA binding is only partially restored. This partial rescue results in inefficient mRNA localization, particularly at early stages of oogenesis. We posit that the artificially dimerized Egl assembles into a conformation that does completely mimic Dlc-mediated dimeric Egl. As such, its capacity to bind mRNA is not fully restored. Thus, Dlc performs an essential

role in facilitating Egl's RNA binding activity. Disrupting this function results in mRNA localization defects and a failure to maintain oocyte fate.

RESULTS

Artificial dimerization of Egl restores BicD binding and partially restores mRNA binding.

We recently demonstrated that Dlc is required for dimerization of Egl (Goldman et al., 2019). An Egl mutant that was unable to interact with Dlc (*egl_2pt*) was not only dimerization defective, it was also compromised for binding mRNA and BicD (Goldman et al., 2019; Navarro et al., 2004). In order to test the hypothesis that Egl dimerization is required for mRNA binding, and consequently associating with BicD, we attached a leucine zipper, a well-characterized dimerization domain, to the C-terminus of *egl_2pt*. This mutant was expressed in S2 cells and tested for mRNA and BicD binding. As expected, Egl_2pt-zip did not bind Dlc, yet due to the presence of the leucine zipper, dimerization was restored (Goldman et al., 2019). Consistent with our hypothesis, using this in vitro assay, mRNA and BicD binding were also restored (Goldman et al., 2019).

Our next objective was to determine whether artificial dimerization could restore Egl function in vivo. Transgenic flies expressing either FLAG or GFP tagged Egl_wt, Egl_wt-zip, Egl_2pt or Egl_2pt-zip were generated. The constructs contained silent mutations that made them refractory to depletion via *egl* shRNA (Sanghavi et al., 2016). This enabled us to generate flies that were depleted of endogenous Egl, yet expressed the transgenic constructs in the germline. For these initial binding experiments, an early-stage Gal4 driver (maternal alpha tubulin-Gal4; Bloomington stock 7063) was used to deplete endogenous Egl. This driver is not active in the germanium but is turned on in early stage egg chambers (Sanghavi et al., 2016). As such, the function of Egl in oocyte specification can be bypassed and mature egg chambers can be generated (Sanghavi et al., 2016), thus enabling us to perform the binding experiments.

We first tested the ability of these constructs to bind BicD and Dlc using a co-immunoprecipitation assay. Ovarian lysates were prepared from flies expressing GFP tagged Egl_wt, Egl_2pt, Egl_2pt-zip or Egl_wt-zip. The tagged proteins were immunoprecipitated using GFP-trap beads and the co-precipitating BicD and Dlc were analyzed using their corresponding antibodies. As expected, Egl_2pt displayed reduced binding to both Dlc and BicD (Fig. 1A, B). Although Egl_2pt-zip was still unable to bind to Dlc, its ability to associate with BicD was restored (Fig. 1A, B). Addition of the zipper to wild-type Egl did not enhance or diminish its ability to bind either BicD or Dlc (Fig. 1A, B). Thus, this approach revealed that artificial dimerization of Egl_2pt restores BicD binding.

We next examined RNA binding using a well characterized assay (Dienstbier et al., 2009). This assay involves tethering RNA localization elements to beads using a streptavidin-binding aptamer (Dienstbier et al., 2009). Beads bounds with the *ILS* localization element from the *I factor* retrotransposon were incubated with ovarian lysates from flies expressing the indicated constructs. Consistent with our published results (Goldman et al., 2019), Egl_2pt displayed reduced RNA binding in comparison to wild-type Egl (Fig. 1C, D). By contrast, using this assay, Egl_2pt-zip bound to the *ILS* localization element at the same level as Egl_wt (Fig. 1C, D). Similar results were

obtained using localization elements from *K10* mRNA (*TLS*) and *grk* mRNA (*GLS*) (Supplemental Fig. 1 A, B).

In order to examine the ability of the Egl to associate with native mRNAs, we immunoprecipitated the respective constructs from ovarian lysates, extracted bound mRNAs, and determined their abundance using reverse transcription followed by quantitative PCR (IP RT-qPCR). For this analysis, we determined the level of *gurken* (*grk*), *nanos* (*nos*), *polar granule component* (*pgc*), *mutator2* (*mu2*) and *dacapo* (*dap*) that co-precipitated with Egl. The binding of these cargoes were normalized to *gamma tubulin* and *rp49* mRNA, both of which precipitate non-specifically with beads. In comparison to Egl_wt, all five cargoes displayed reduced binding to Egl_2pt (Fig. 1E). In addition, with all five cargoes, partial restoration of binding was observed using Egl_2pt-zip (Fig. 1E). However, the rescue was not complete (Fig. 1E). Thus, using this assay, artificial dimerization of Egl does not completely rescue the mRNA binding function of Egl_2pt.

It was somewhat surprising that the in vitro and in vivo assays produced slightly different results. The most direct comparison can be made using the *GLS* localization element from *grk* mRNA. Using the in vitro aptamer-based assay, Egl_2pt displays a ten fold mRNA binding deficit for this localization element, whereas in the context of the native mRNA, the binding deficit is closer to two fold. In addition, although full rescue of RNA binding is observed with Egl_2pt-zip using the in vitro assay, this is not the case in vivo (Supplemental Fig. 1B and Fig. 1E). As will be shown in subsequent sections, oocyte specification and mRNA localization phenotypes are more consistent with the in vivo (IP RT-qPCR) result.

Egl dimerization is required for meiosis restriction.

Oocyte specification occurs within the germanium. A cystoblast is produced at the distal tip of the germarium via division of a germline stem cell. The cystoblast replicates four times to generate a cyst containing sixteen interconnected cells. Within this early cyst, two cells initiate a meiotic program as evident by the formation of the synaptonemal complex. As the cyst matures, one of these cells will be specified as the oocyte and will retain the synaptonemal complex. The other cell will eventually exit meiosis and revert to a nurse cell fate (Hughes et al., 2018; Huynh and St Johnston, 2004) (Fig. 2A). Specification of the oocyte is defective in null alleles of *egl* (Carpenter, 1994; Theurkauf et al., 1993). In fact, in these mutants, numerous cells within the cyst initiate a meiotic program and form a synaptonemal complex. However, this effect is temporary; meiosis is eventually terminated in all cells of the cyst and an oocyte is never specified (Carpenter, 1994; Huynh and St Johnston, 2000).

In order to examine this process in our mutants, germaria were stained using an antibody against C(3)G, a component of the synaptonemal complex (Page and Hawley, 2001). Endogenous Egl was depleted in the germanium using the *nanos*-Gal4 driver (Bloomington stock #4937). The same driver was also responsible for expressing transgenic wild-type or mutant constructs. A phenotype similar to the null was observed in *egl_2pt* mutants. Like the null allele, in *egl_2pt* mutants, numerous cells within the

cyst inappropriately entered meiosis. However, as with the nulls, this effect was transient, and by stage1, the synaptonemal complex was either undetected or present as faint residual puncta (Fig. 2B, C, D, D', G). This phenotype was significantly restored in flies expressing Egl_2pt-zip and 73% of germaria displayed normal synaptonemal complex formation in stage1 egg chamber (Fig. 2E, G). However, the rescue was not complete and 21% of egg chambers displayed fragmented C(3)G staining (Fig. 2F, F', G). Based on these results, we conclude that proper progression of meiosis requires Dlc-mediate Egl dimerization and that artificial dimerization Egl is able to partially compensate for loss of Dlc binding.

Oocyte specification requires Egl dimerization.

We next examined the specification of oocyte fate by determining the localization of Orb in the germarium and early stage egg chambers. Orb, the *Drosophila* ortholog of Cytoplasmic Polyadenylation Element Binding Protein 1, is enriched within the two cells that initially enter meiosis. Subsequently, Orb becomes highly enriched within the oocyte, and is therefore a useful marker of oocyte fate specification and maintenance (Huynh and St Johnston, 2000; Lantz et al., 1994). In contrast to egg chambers expressing Egl_wt or Egl_wt-zip, Orb is never localized to a single cell with the germaria of Egl_2pt mutants (Fig. 3A, B, D, G). This phenotype is partially restored in Egl_2pt-zip flies, and about 30% of ovarioles proceed though normal development (Fig. 3C, F, G). However, in about 60% of ovarioles, the oocyte is either not specified, or if specification does occur, oocyte fate is not maintained (Fig. 3E, G). Thus, Dlc-mediated dimerization of Egl is required for specification and maintenance of oocyte fate, and artificial dimerization of Egl is only able to partially rescue this phenotype.

Efficient mRNA localization requires Egl dimerization.

Several mRNA's that are localized by an Egl-dependent mechanism are known to be enriched within the presumptive oocyte (Kasravi et al., 1999; Roth et al., 1995). For this analysis, we examined the localization of *grk* and *mu2* within the germarium and early stage egg chambers. Both cargoes were highly enriched within a single cell of stage1 and stage2 egg chambers in files expressing Egl_wt (Fig. 4A, A', D, D' arrow). A similar pattern was observed in Egl_wt-zip egg chambers (Supplemental Fig. 1E, F). By contrast, both mRNAs were completely delocalized in Egl_2pt mutants (Fig. 4B, B', E, E'). In flies expressing Egl_2pt-zip, a modest enrichment of *grk* and *mu2* mRNA could be detected within the oocyte of stage1 and stage2 egg chambers (Fig. 4C, C', F, F', dashed outline). However, quantification of oocyte enrichment revealed that this rescue was only partial (Fig. 4M, N). Thus, efficient localization of these mRNAs requires Dlc-mediated Egl dimerization. Artificial dimerization is only able to partially substitute for Dlc.

In contrast to these mRNAs, Dynein was less dependent on Egl's ability to dimerize for its oocyte enrichment. Dynein could be detected within a single cells in stage1 egg chambers in flies expressing Egl_2pt (Supplemental Fig. 1C). However, this enrichment was reduced in stage2 egg chambers, coincident with loss of oocyte fate (Supplemental Fig. 1C'). In egg chambers expressing Egl_2pt-zip, Dynein was either normally localized within the oocyte (Supplemental Fig. 2D, D', arrow) or became delocalized in those egg

chambers in which oocyte fate was lost (Supplemental Fig. 2D, asterisk). Thus, it appears that irrespective of Egl dimerization, as long as oocyte fate is maintained, Dynein is able to localize normally within the oocyte.

Next, we examined the localization of these cargoes in mid-stage egg chambers. For this experiment, endogenous Egl was depleted using the afore mentioned early stage driver (maternal alpha tubulin-Gal4; Bloomington stock 7063). This bypasses the function of Egl in the germarium and early stage egg chambers. The same driver was also responsible for expressing the transgenic constructs. *grk* mRNA is localized at the dorsal anterior corner of stage10 egg chambers (Neuman-Silberberg and Schupbach, 1993). This pattern was observed in egg chambers expressing Egl_wt or Egl_wt-zip (Fig. 4G, data not shown). *grk* mRNA was still enriched at the dorsal-anterior corner of egg chambers expressing Egl_2pt. However, the level of enrichment was reduced in comparison to the wild-type control (Fig. 4H, O). This phenotype was only partially rescued in flies expressing Egl_2pt-zip (Fig. 4I, O).

mu2 mRNA has been shown to localize to the anterior cortex of stage10 egg chambers (Kasravi et al., 1999). However, the localization of this mRNA has not yet been described using single molecule fluorescent in situ hybridization (smFISH). We show here that *mu2* mRNA localizes to numerous discrete puncta along the anterior margin of the oocyte in flies that are either completely wild-type or in flies depleted of endogenous Egl and expressing Egl_wt-FLAG (Fig. 4J, data not shown). The same pattern is observed in flies expressing Egl_wt-zip (data not shown). In flies expressing Egl_2pt, *mu2* puncta are often delocalized from the anterior margin of the oocyte (Fig. 4K, P). The anterior localization of this mRNA was mostly restored in flies expressing Egl_2pt-zip (Fig. 4L, P).

We can make two conclusions based on these results. First, mRNA localization at early stages of oogenesis is highly dependent on Dlc-mediated Egl dimerization. Artificial dimerization of Egl is not capable of fully rescuing these early phenotypes. Second, at mid-stages of oogenesis, mRNA localization is less affected by Egl dimerization. Even in the absence of Egl-dimerization, *grk* and *mu2* mRNA remained relatively localized. Distinct mechanisms of localization might be active in early and mid stage egg chambers. If true, this would account for the different localization phenotypes observed for *grk* and *mu2* mRNA in early vs mid-stage egg chambers. Future studies will be critical to reveal these potentially distinct mechanisms.

DISCUSSION

Navarro and colleagues demonstrated several years ago that Egl contains a Dlc-interaction motif within its C-terminus (Navarro et al., 2004). They further showed that point mutations within this region, which they referred to as *egl_2pt*, resulted in oocytes specification defects (Navarro et al., 2004). At that time, the role of Dlc in this pathway was unclear, and it was suggested that Dlc might serve as a way to link Egl and its associated mRNA cargo with the Dynein motor. Subsequent research has shown that the actual link between Egl and Dynein is the adaptor protein, BicD (McClintock et al., 2018; Sladewski et al., 2018). We recently demonstrated that the role of Dlc in this pathway is to facilitate dimerization of Egl, a pre-requisite for efficient mRNA binding (Goldman et al., 2019).

Although initially identified as a component of the Dynein motor, Dlc (also known as LC8) has been shown to interact with numerous proteins. In fact, three hundred nineteen interactions are listed for human LC8 and sixty three interactions are listed for *Drosophila* Dlc on BioGRID. The emerging picture suggests that the main role for Dlc is to facilitate the dimerization of proteins, in particular those that harbor regions of low complexity or intrinsically disordered stretches (Barbar, 2008; Reardon et al., 2020). Apart from its central RNA binding domain, Egl contains large stretches of low complexity regions and a single consensus Dlc-interaction motif at its C-terminal end (Navarro et al., 2004). Although structural information is not yet available regarding the mechanism of Egl dimerization, it is tempting to speculate that Dlc-mediated dimerization alters the conformation of Egl's RNA binding domain in such a way as to promote efficiently cargo binding.

Egl is thought to be the primary mRNA adaptor for the Dynein motor in *Drosophila* oocytes and embryos (Dienstbier et al., 2009; Vazquez-Pianzola et al., 2017). As such, it has to be able to bind diverse cargo. In select cases, it has been demonstrated that Egl recognized a secondary structure in its target mRNAs (Dienstbier et al., 2009; Vazquez-Pianzola et al., 2017). However, whether comparable structures are present in all Egl mRNA cargo is not known. Thus, having an RNA binding domain that is somewhat flexible and unstructured might be required for Egl to recognize diverse cargo. Dlc-mediated dimerization might in turn impose some structural rigidity to the complex such that only mRNAs destined for localization are coupled to Dynein.

Our results indicate that artificial dimerization of Egl is able to partially substitute for Dlc in this pathway. The reason for this incomplete rescue might have to do with the three dimensional conformation of the complex. In our construct, the leucine zipper is placed at the C-terminus of Egl, and therefore dimerization is induced at this site. The structure of the resulting complex might not be identical to the dimeric structure that is produced via Dlc-mediated dimerization. As such, the RNA binding domain of Egl might not adopt an optimal conformation, thus resulting in inefficient cargo binding and Dynein mediated transport.

Consistent with this notion, BicD and Glued (a component of the Dynactin complex) co-localized on microtubule filaments in egg chambers treated with PIPES, indicating

active Dynein mediated transport of BicD-linked cargo (Supplemental Fig. 2A). By contrast, although Glued still localizes to filaments in Egl_2pt egg chambers, BicD was more diffusely localized (Supplemental Fig. 2B), suggesting defective transport of BicD-linked cargo. Filament localization was only partially rescued in egg chambers expressing Egl_2pt-zip (Supplemental Fig. 2C). Thus, although artificial dimerization is able to restore the Egl-BicD interaction, this complex does not efficiently associate with Dynein.

Recently, Panoramix (Panx), a protein that functions in the piRNA pathway was also shown to dimerize in a Dlc-dependent manner (Evelyn L. Eastwood, 2021; Jakob Schnabl, 2021). Artificial dimerization of a *panx* mutant that could no longer interact with Dlc restored the function of *panx*. Similar to our findings, the rescue of certain *panx* mutant phenotypes was incomplete (Jakob Schnabl, 2021).

ACKNOWLEDGEMENTS

We are grateful to Simon Bullock for providing the *ILS* and *TLS* aptamer constructs and Scott Hawley for providing the C(3)G antibody. We would also like to thank Vladimir Gelfand for providing the Glued antibody. We are grateful to the Bloomington Stock Center, Developmental Studies Hybridoma Bank, and the *Drosophila* Genomics Resource Center for providing fly strains, antibodies, cell lines, and DNA constructs. This work was supported by a grant from the National Institutes of Health to G.B.G (R01GM100088).

MATERIALS AND METHODS

Fly stocks and DNA constructs

The following shRNA stocks were used:
egl shRNA-1 (Bloomington stock center; #43550, donor TRiP).

shRNA expression was driven using:
P{w[+mC]=matalpha4-GAL-VP16}V37 (Bloomington Stock Center, #7063; donor Andrea Brand) for early-stage expression.
P{w[+mC]=GAL4::VP16-nos.UTR}CG6325[MVD1] (Bloomington Stock center, #4937; donor Ruth Lehmann) for expression in the germanium.

Vectors expressing Egl_wt and Egl_2pt were designed in a previous study (Goldman et al., 2019). The expression of these constructs were driven using a maternal promoter. For this study, the coding regions from those constructs were sub-cloned into the the pUASp-attB-K10 vector (Koch et al., 2009) containing either a C-terminal GFP tag or 3xFLAG tag. The leucine zipper from yeast GCN4 (AAL09032.1) along with a preceding flexible linker sequence was synthesized with *Drosophila* codon optimization by Genewiz. The zipper was cloned downstream of the GFP or FLAG tag. The GFP tagged transgenic constructs were inserted at the ZH-86Fa site (Bloomington stock center; #24486, donor Konrad Basler & Johannes Bischof) and the FLAG tagged constructs were inserted at su(Hw)attP1 site (Bloomington stock center; #34760, donor Norbert Perrimon). The strains were injected by BestGene Inc. Fly stocks and crosses used for these experiments were maintained at 25^0C. The *ILS* and *TLS* aptamers were a gift from Simon Bullock. The *GLS* aptamer construct was created using Gibson assembly (NEB). The *GLS* sequence was synthesized by Genewiz and this double stranded DNA was used to replace the *ILS* sequence in the *ILS* aptamer vector.

Antibodies

The following antibodies were used: anti-FLAG (Sigma Aldrich, F1804, 1:5000 for western, 1:500 for immunofluorescence), mouse anti-BicD (Clones 1B11 and 4C2, Developmental Studies Hybridoma Bank, 1:30 for immunofluorescence; 1:300 for western, donor R. Steward), rabbit anti-Ctp (Abcam, ab51603, 1:5000 for western), GFP nanobody booster (Chromotek; 1:500 for immunofluorescence), mouse anti-GFP (Clontech, JL-8, 1:5000 for western), rabbit anti-GFP (Chromotek; 1:3000 for immunofluorescence), C3G (generous gift from S. Hawley, mouse anti-C(3)G, 1:500), Orb (mouse anti-Orb, clone 4H8, 1:30 dilution), mouse anti-Dhc (Developmental Studies Hybridoma Bank, clone 2C11-2, 1:50; for immunofluorescence, donor J. Scholey), rabbit anti-Glued (generous gift from V. Gelfand, 1:500 for immunofluorescence). The following secondary antibodies were used: goat anti-rabbit Alexa 594, 555 and 488 (Life Technologies, 1:400, 1:400 and 1:200 respectively); goat anti-mouse Alexa 594, 555 and 488 (Life Technologies, 1:400 , 1:400 and 1: 200 respectively) goat anti-mouse HRP (Pierce, 1:5000); and goat anti-rabbit HRP (Pierce, 1:5000).

RNA binding studies

The in vitro RNA binding experiments using *ILS*, *TLS* and *GLS* localization elements were performed as previously described (Dienstbier et al., 2009; Goldman et al., 2019).

In brief, 5µg of RNA was refolded in 10µL of *Drosophila* extraction buffer (DXB: 25mM HEPES pH 6.5, 50mM KCl, 1mM MgCl2, 250mM sucrose, 0.05% NP40, supplemented with 10µM MgATP and 1mM DTT at the time of use). The refolded RNA was next incubated with High Capacity Streptavidin Agarose Beads (Pierce) in 90µL DXB for 1.5 hours at 4°C while nutating. Extracts from frozen *Drosophila* ovaries were prepared using lysis buffer (50mM Tris pH 7.5, 200mM NaCl, 0.2mM EDTA, 0.05% NP40, Halt protease inhibitor cocktail, Pierce). 600ug of total protein was used in each binding experiment. Extracts were incubated with the RNA-bound streptavidin beads for 15 min at room temperature followed by 30 min at 4°C with nutation. The beads were then washed 4 times in lysis buffer, the bound proteins were eluted by boiling in Laemmli buffer and examined by western blotting.

The binding of Egl constructs to native mRNAs from ovaries was analyzed as previously described (Goldman et al., 2019). Briefly, 600ug of lysate was used in each immunoprecipitation. The tagged proteins were immunoprecipitated using FLAG M2 antibody beads (Sigma). Co-precipitating RNAs were reverse transcribed using random hexamers and Superscript III (Life Technologies). Quantitative (qPCR) was performed using SsoAdvanced Universal SYBR Green Supermix (Bio-Rad). A Bio-Rad CFX96 Real-Time PCR System was used for this experiment. Fold enrichment was calculated by comparing ct values for each RNA to that obtained for *γ-tubulin* and *rp49*.

Protein-protein interaction

A co-immunoprecipitation experiment was used to analyze protein-protein interaction (Goldman et al., 2019). In brief, ovaries were homogenized into lysis buffer (50mM Tris pH 7.5, 200mM NaCl, 0.2mM EDTA, 0.05% NP40 and Halt protease inhibitor cocktail, Pierce) and cleared by centrifugation at 10,000g at 4^0C for 5min. 1mg of total protein was used per immunoprecipitation. Immunoprecipitation was performed by incubating lysates at 4^0C for 1hour with GFP-trap beads (Chromotek). Next, the beads were washed four times with lysis buffer. Co-precipitating proteins were eluted in Laemmli buffer, run on a gel, and analyzed by western blotting.

Immunofluorescence and in situ hybridization

Immunofluorescence and in situ hybridization were performed as previously described (Goldman et al., 2019). Ovaries were dissected and fixed in 4% formaldehyde (Pierce) for 20 min at room temperature. For immunofluorescence experiments, primary antibody was incubated in blocking buffer (PBS + 0.1% Triton X-100 + 2% BSA) overnight at 4°C. The next day, the samples were washed three times in PBST (PBS + 0.1% Triton X-100) and incubated overnight with the fluorescent secondary antibody in the same blocking buffer. The samples were then washed four times with PBST, stained with DAPI, and mounted onto slides using Prolong Diamond (Life technologies). For in situ hybridization, the ovaries were dissected and fixed as above. After fixation, ovaries were stored in in 100% methanol at -20°C for 1 hour. Next, the samples were re-hydrated with three 10 min washes using a solution of PBST and 100% methanol (3:7, 1:1, 7:3) and rinsed four times with PBST. The hydrated samples were next washed for 10 minutes in Wash Buffer (4xSSC, 35% deionized formamide, 0.1% Tween-20). Fluorescent oligo probes (Stellaris probes) were obtained from Biosearch technologies.

Fluorescent probes diluted in Hybridization Buffer (10% dextran sulfate, 0.1mg/ml salmon sperm ssDNA, 100 μl vanadyl ribonucleoside (NEB biolabs), 20ug/ml RNAse-free BSA, 4x SSC, 0.1% Tween-20, 35% deionized formamide) were added to the ovaries and incubated overnight at 37°C. The following day, the samples were washed twice with pre-warmed Wash Buffer for 30 min. After two rinses with PBST and two rinses with PBS, the samples were counter-stained with DAPI, and mounted onto slides using Prolong Diamond.

Microscopy

Images were captured on either a Zeiss LSM 780 inverted confocal microscope or an inverted Leica Stellaris confocal microscope. Images were processed for presentation using Fiji, Adobe Photoshop, and Adobe Illustrator. All imaging experiments were performed at the Augusta University Cell Imaging Core.

Quantification

All western blot images were acquired on a Bio Rad ChemiDoc MP. Band intensities were quantified using the Bio Rad Image lab software. RNA and protein enrichment was quantified by measuring the average pixel intensity of the localized signal and dividing by the average pixel intensity of the delocalized signal. For quantifying stage2 oocyte enrichment, the localized signal in the oocyte was compared to the average signal in the rest of the egg chamber. In mid-stage egg chamber, the localized signal for *grk* mRNA at the dorsal-anterior corner was compared to the delocalized signal in the rest of the oocyte. In order to stay consistent between images, the focal plan containing the karyosome of the oocyte nucleus was used for *grk* signal quantification. The above quantifications were performed using the Zeiss Zen Black software. For quantification of *mu2* signal, an 8 micron z stack was analyzed for each sample. The mid-saggital plane of the egg chamber was used as the center and 4 focal planes above and below were imaged. A maximum projection image was then generated and delocalized particles were counted. Localized particles were considered to be within 20 microns from the anterior margin of the oocyte. The remainder of the particles were considered to be delocalized. The particle analysis tool in Fiji was used for this quantification. Graphs were assembled using Graphpad Prism9.

FIGURE LEGENDS

Figure 1: Artificial dimerization of Egl. (A) A co-immunoprecipitation experiment was performed using ovarian lysates from flies expressing Egl_wt-GFP, Egl_wt-zip-GFP, Egl_2pt-GFP, and Egl_2pt-zip-GFP. The lysates were incubated with GFP-Trap beads and after binding and wash steps, the bound proteins were eluted in SDS buffer. Eluates were analyzed by western blotting using the indicated antibodies. Total and IP fractions are shown. **(B)** The data from three independent co-immunoprecipitation experiments were quantified. Binding is shown relatively to the BicD and Dlc value obtained with the Egl_wt sample. Neither Egl_2pt nor Egl_2pt-zip is able to associate with Dlc. However, as a consequence of artificial dimerization, the binding to BicD is restored with Egl_2pt-zip. **(C)** Ovarian lysates from the indicated strains were used in an in vitro RNA binding assay. The lysates were incubated with Streptavidin beads coated with the *ILS* localization element. Bound proteins were eluted and analyzed by western blotting. Total and bound fractions are shown. **(D)** Data from three independent *ILS* binding experiments were quantified. Binding was normalized to the level observed in the Egl_wt sample. Using this in vitro assay, artificial dimerization of Egl restores the mRNA binding defect. **(E)** Ovarian lysates from the indicated strains were prepared and the tagged proteins were immunoprecipitated using FLAG antibody beads. Bound mRNAs were extracted and analyzed by reverse transcription followed by quantitative PCR (RTqPCR) using primers against *grk*, *nos*, *mu2*, *dap* and *pgc*. RNA enrichment was normalized relative to the amount of *gamma tubulin* and *rp49* mRNAs that co-precipitated with the beads. Binding was normalized to the level of mRNA enrichment detected with Egl_wt. Using this assay, artificial dimerization of Egl only partially restored the RNA binding deficit. For the BicD/Dlc interaction, a two-way ANOVA with Tukey's multiple comparison correction was used. For the *ILS* binding experiment, an Unpaired *t*-test was used and for the RTqPCR experiment, a one-way ANOVA with Tukey's multiple comparison correction was used. ****p<0.0001, *** p<0.001, ** p<0.01, *p<0.05, ns = not significant.

Figure 2: Artificial dimerization partially restores the meiosis defect of Egl_2pt mutants. (A) A schematic of the *Drosophila* germarium and early stage egg chambers. Germline stem cells, the synaptonemal complex, and the localization of Orb are indicated. **(B-G)**. Ovaries from flies expressing Egl_wt, Egl_2pt, or Egl_2pt-zip were fixed and processed for immunofluorescence using an antibody against C(3)G, a marker for the synaptonemal complex (red). The tissues were also counter-stained with Phalloidin to reveal the actin cytoskeleton (green). In flies expressing Egl_wt, 100% of ovarioles contained C(3)G staining within one cell of stage1 egg chambers (B, G). By contrast, ovarioles from Egl_2pt mutants either lacked C3G staining in stage1 egg chambers and beyond (C, G), or displayed residual puncta of C(3)G (D, D', G). In flies expressing Egl_2pt-zip, the vast majority displayed normal C(3)G staining in stage1 egg chambers (E, G). However, in 21% of ovarioles, the C(3)G staining in stage1 egg chambers was fragmented (F, F', G). The scale bar is 10 microns.

Figure 3: Oocyte specification and maintenance. (A-G) Ovaries were dissected and fixed from flies expressing Egl_wt, Egl_2pt, Egl_2pt-zip or Egl_wt-zip. The ovaries were processed for immunofluorescence using an antibody against Orb, a protein that is

enriched within the oocyte of stage1 egg chambers and beyond (indicated by arrows in A, C and D). The signal for Orb is shown using a Red to White look up table (LUT). Low intensity pixels are depicted in red whereas high intensity pixels are shown in white. In contrast to egg chambers expressing Egl_wt and Egl_wt-zip, Orb was never localized to a single cell in egg chambers expressing Egl_2pt (A, B, D, G). In flies expressing Egl_2pt-zip, three phenotypes were observed (G). In a small percentage of ovarioles, Orb was not localized to a single cell within stage1 egg chambers. In the remainder of the ovarioles, Orb was either correctly localized throughout egg chamber maturation (F, G) or was initially localized correctly and then became delocalized once oocyte fate was lost (E, G). Thus, artificial dimerization of Egl_2pt partially rescues the oocyte specification and and maintenance defect. The scale bar in A-D is 10 microns. In panel E the scale bar is 20 microns, and 50 microns in panel F.

Figure 4: mRNA localization in early and mid-stage egg chambers. (A-F) Ovaries were dissected and fixed from flies expressing the indicated constructs. The germaria and early stage egg chambers were processed for single molecule fluorescent in situ hybridization (smFISH) using probes against *grk* (A-C) or *mu2* (D-F). The egg chambers were also counterstained with DAPI (shown in greyscale). The in situ signal for *grk* and *mu2* is shown using the same Red to White look up table (LUT) that was used for Orb. The oocyte in C' and F' is indicated with a dashed line. *grk* and *mu2* mRNA are highly enriched in the oocyte in stage1 and 2 wild-type egg chambers but are completely delocalized in Egl_2pt mutants. Both mRNA are partially enriched with the oocyte of flies expressing Egl_2pt-zip. **(G-L)** Ovaries from the same strains were processed for smFISH using probes against *grk* (G-I) and *mu2* (J-L). Stage10 egg chambers were imaged for these experiments. The in situ signal is depicted using the Red to White look up table (LUT). The egg chambers were also counterstained with DAPI (cyan). Panels J-L represent a maximum projection of a 8 micron section centered around the mid-saggital plane of the egg chamber. *grk* mRNA localized to the dorsal anterior corner in strains expressing Egl_wt. Although a similar pattern was observed in egg chambers expressing Egl_2pt and Egl_2pt-zip, the level of dorsal-anterior enrichment was reduced. *mu2* mRNA localized as distinct particles at the anterior margin of stage 10 egg chambers in flies expressing Egl_wt or Egl_2pt-zip. However, in flies expressing Egl_2pt, numerous delocalized particles were observed. **(M-N)** Quantification of oocyte enrichment of *grk* (M) and *mu2* (N) mRNA in stage1 egg chambers. An unpaired *t*-test for used for this analysis **(O)** Quantification of dorsal-anterior enrichment of *grk* mRNA in the indicated strains. **(P)** Quantification of delocalized *mu2* foci in the indicated strains. A One-way ANOVA with Tukey's multiple comparison correction was used for panels O and P. ****p<0.0001, *** p<0.001, ** p<0.01, ns = not significant. The scale bar in A-F is 10 microns and in G-L the scale bar is 50 microns.

Supplemental Figure 1: (A-B) Ovarian lysates from the indicated genotypes were prepared and used in an in vitro RNA binding experiment using the *TLS* (A) or *GLS* (B) localization elements. The bound proteins were eluted and analyzed by western blotting using the FLAG antibody. Total and bound fractions are shown. **(C-D)** Localization of Dynein heavy chain (Dhc, red) in strains expressing Egl_2pt (C, C') or Egl_2pt-zip (D, D'). The egg chambers in panel C were also counterstained with DAPI (shown in

greyscale). The enrichment of Dhc within the oocyte is indicated by the arrow. The asterisk indicated egg chambers that have lost oocyte fate. **(E-F)** Egg chambers from Egl_wt-zip are shown. The egg chambers were processed for smFISH using probes against *grk* (E, E') or *mu2* (F, F'). The scale bar in D' is 50 microns. In the rest of the images, the scale bar is 20 microns.

Supplemental Figure 2: (A-C) Egg chambers from the indicated genotypes were incubated with PIPES prior to fixation. Egg chambers were processed for immunofluorescence using antibodies against BicD (green) and Glued (red). A merged image is also shown. BicD and Glued co-localize on microtubule filaments in strains expressing Egl_wt (A). By contrast, BicD did not display a filamentous localization pattern in Egl_2pt egg chambers (B). Egl_2pt-zip produced an intermediate phenotype and partial filament localization of BicD could be observed (C). The scale bar is 50 microns.

Bibliography

1. Barbar, E., 2008. Dynein light chain LC8 is a dimerization hub essential in diverse protein networks. Biochemistry 47, 503-508.
2. Carpenter, A.T., 1994. Egalitarian and the choice of cell fates in Drosophila melanogaster oogenesis. Ciba Found Symp 182, 223-246; discussion 246-254.
3. Dienstbier, M., Boehl, F., Li, X., Bullock, S.L., 2009. Egalitarian is a selective RNA-binding protein linking mRNA localization signals to the dynein motor. Genes Dev 23, 1546-1558.
4. Evelyn L. Eastwood, K.A.J., Susanne Bornelöv, Marzia Munafò, Vasileios Frantzis, Emma Kneuss, Elisar J. Barbar, Benjamin Czech, Gregory J. Hannon, 2021. Dimerisation of the PICTS complex via LC8/Cut-up drives co-transcriptional transposon silencing in Drosophila. bioRxiv 2021.01.08.425839.
5. Goldman, C.H., Gonsalvez, G.B., 2017. The Role of Microtubule Motors in mRNA Localization and Patterning Within the Drosophila Oocyte. Results Probl Cell Differ 63, 149-168.
6. Goldman, C.H., Neiswender, H., Veeranan-Karmegam, R., Gonsalvez, G.B., 2019. The Egalitarian binding partners Dynein light chain and Bicaudal-D act sequentially to link mRNA to the Dynein motor. Development 146.
7. Hoogenraad, C.C., Akhmanova, A., 2016. Bicaudal D Family of Motor Adaptors: Linking Dynein Motility to Cargo Binding. Trends Cell Biol 26, 327-340.
8. Hughes, S.E., Miller, D.E., Miller, A.L., Hawley, R.S., 2018. Female Meiosis: Synapsis, Recombination, and Segregation in Drosophila melanogaster. Genetics 208, 875-908.
9. Huynh, J.R., St Johnston, D., 2000. The role of BicD, Egl, Orb and the microtubules in the restriction of meiosis to the Drosophila oocyte. Development 127, 2785-2794.
10. Huynh, J.R., St Johnston, D., 2004. The origin of asymmetry: early polarisation of the Drosophila germline cyst and oocyte. Curr Biol 14, R438-449.
11. Jakob Schnabl, J.W., Ulrich Hohmann, Maja Gehre, Julia Batki, Veselin I. Andreev, Kim Purkhauser, Nina Fasching, Peter Duchek, Maria Novatchkova, Karl Mechtler, Clemens Plaschka, Dinshaw J. Patel, Julius Brennecke, 2021. The molecular principles of Piwi-mediated co-transcriptional silencing through the dimeric SFiNX complex. bioRxiv 2021.01.08.425619.
12. Kasravi, A., Walter, M.F., Brand, S., Mason, J.M., Biessmann, H., 1999. Molecular cloning and tissue-specific expression of the mutator2 gene (mu2) in Drosophila melanogaster. Genetics 152, 1025-1035.
13. Koch, R., Ledermann, R., Urwyler, O., Heller, M., Suter, B., 2009. Systematic functional analysis of Bicaudal-D serine phosphorylation and intragenic suppression of a female sterile allele of BicD. PLoS One 4, e4552.
14. Lantz, V., Chang, J.S., Horabin, J.I., Bopp, D., Schedl, P., 1994. The Drosophila orb RNA-binding protein is required for the formation of the egg chamber and establishment of polarity. Genes Dev 8, 598-613.
15. Mach, J.M., Lehmann, R., 1997. An Egalitarian-BicaudalD complex is essential for oocyte specification and axis determination in Drosophila. Genes Dev 11, 423-435.
16. McClintock, M.A., Dix, C.I., Johnson, C.M., McLaughlin, S.H., Maizels, R.J., Hoang, H.T., Bullock, S.L., 2018. RNA-directed activation of cytoplasmic dynein-1 in reconstituted transport RNPs. Elife 7.
17. Navarro, C., Puthalakath, H., Adams, J.M., Strasser, A., Lehmann, R., 2004. Egalitarian binds dynein light chain to establish oocyte polarity and maintain oocyte fate. Nat Cell Biol 6, 427-435.
18. Neuman-Silberberg, F.S., Schupbach, T., 1993. The Drosophila dorsoventral patterning gene gurken produces a dorsally localized RNA and encodes a TGF alpha-like protein. Cell 75, 165-174.
19. Page, S.L., Hawley, R.S., 2001. c(3)G encodes a Drosophila synaptonemal complex protein. Genes Dev 15, 3130-3143.

20. Rapali, P., Szenes, A., Radnai, L., Bakos, A., Pal, G., Nyitray, L., 2011. DYNLL/LC8: a light chain subunit of the dynein motor complex and beyond. FEBS J 278, 2980-2996.
21. Reardon, P.N., Jara, K.A., Rolland, A.D., Smith, D.A., Hoang, H.T.M., Prell, J.S., Barbar, E.J., 2020. The dynein light chain 8 (LC8) binds predominantly "in-register" to a multivalent intrinsically disordered partner. J Biol Chem 295, 4912-4922.
22. Roth, S., Neuman-Silberberg, F.S., Barcelo, G., Schupbach, T., 1995. cornichon and the EGF receptor signaling process are necessary for both anterior-posterior and dorsal-ventral pattern formation in Drosophila. Cell 81, 967-978.
23. Sanghavi, P., Liu, G., Veeranan-Karmegam, R., Navarro, C., Gonsalvez, G.B., 2016. Multiple Roles for Egalitarian in Polarization of the Drosophila Egg Chamber. Genetics 203, 415-432.
24. Sladewski, T.E., Billington, N., Ali, M.Y., Bookwalter, C.S., Lu, H., Krementsova, E.B., Schroer, T.A., Trybus, K.M., 2018. Recruitment of two dyneins to an mRNA-dependent Bicaudal D transport complex. Elife 7.
25. Suter, B., 2018. RNA localization and transport. Biochim Biophys Acta Gene Regul Mech 1861, 938-951.
26. Theurkauf, W.E., Alberts, B.M., Jan, Y.N., Jongens, T.A., 1993. A central role for microtubules in the differentiation of Drosophila oocytes. Development 118, 1169-1180.
27. Vazquez-Pianzola, P., Schaller, B., Colombo, M., Beuchle, D., Neuenschwander, S., Marcil, A., Bruggmann, R., Suter, B., 2017. The mRNA transportome of the BicD/Egl transport machinery. RNA Biol 14, 73-89.
28. Weil, T.T., 2014. mRNA localization in the Drosophila germline. RNA Biol 11, 1010-1018.

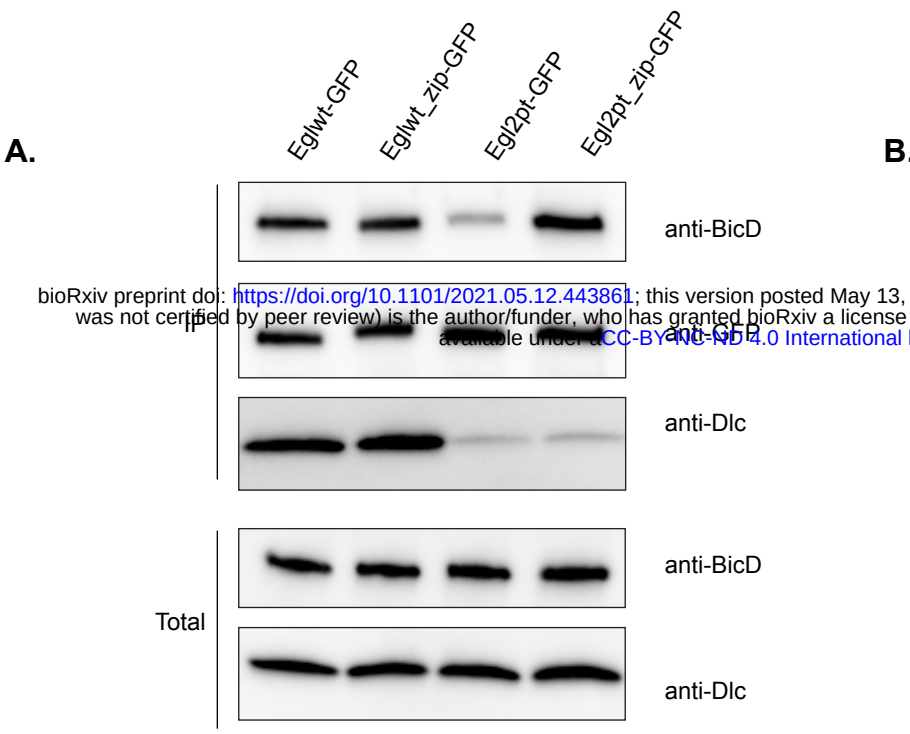

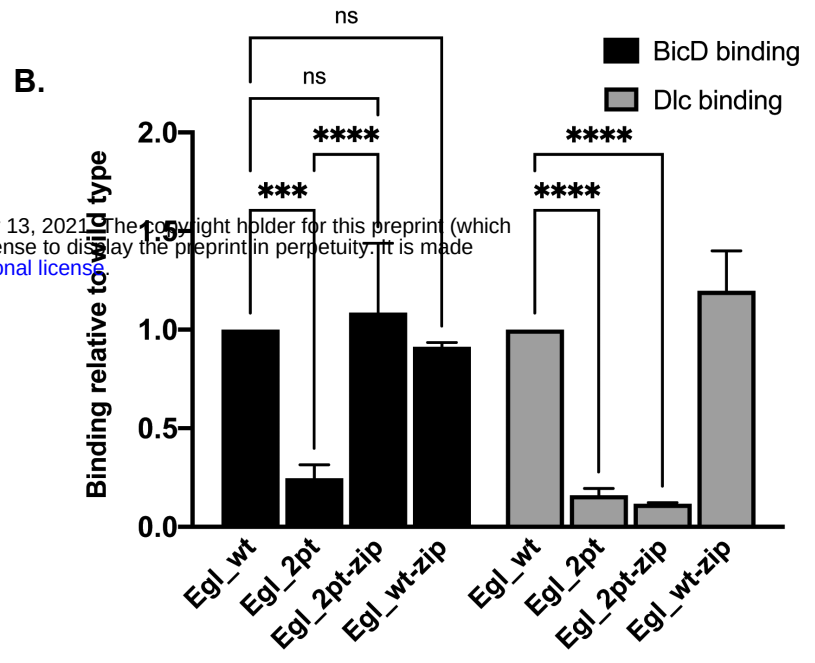

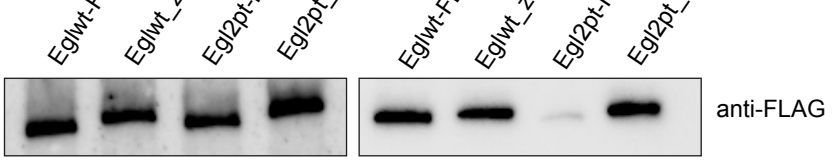

Figure 1

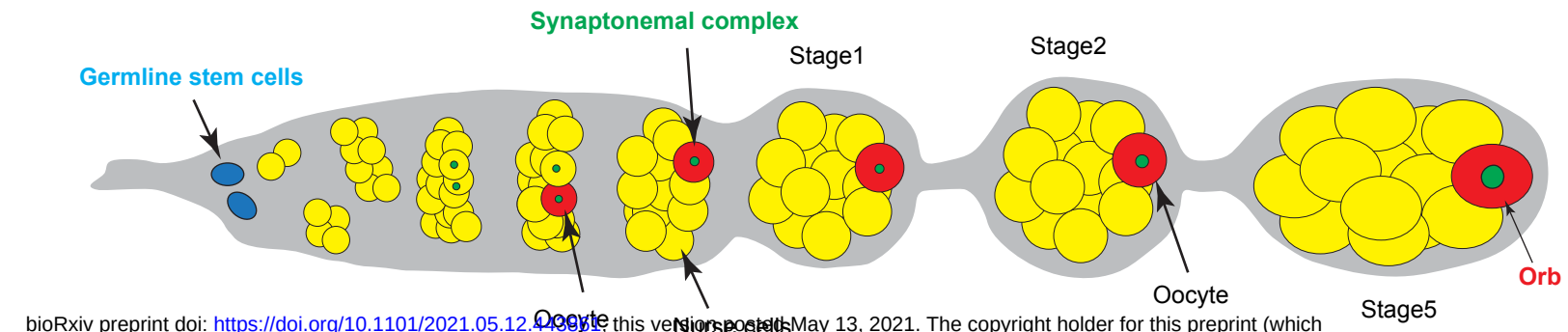

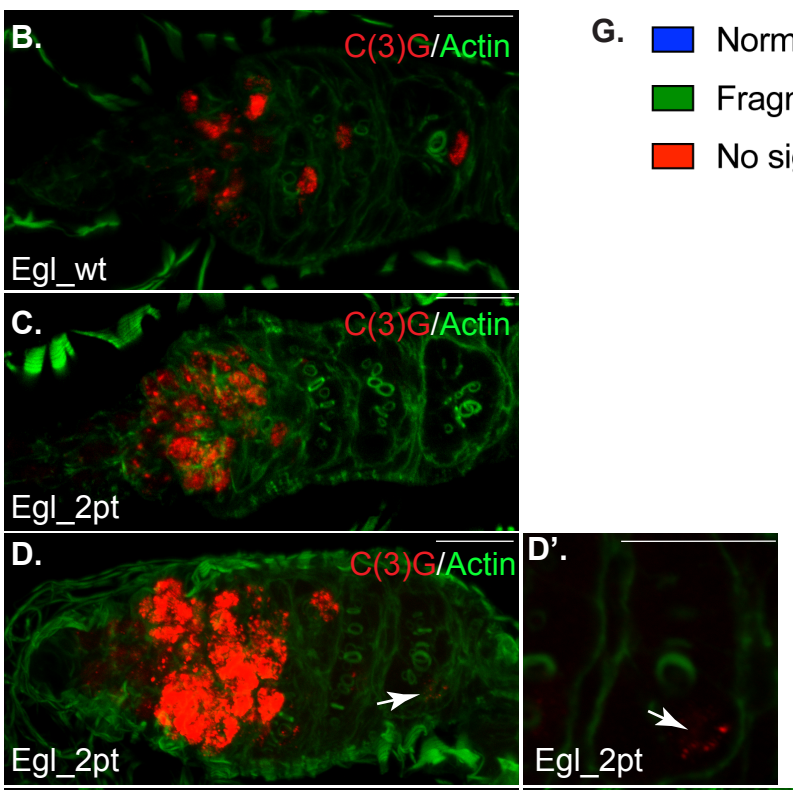

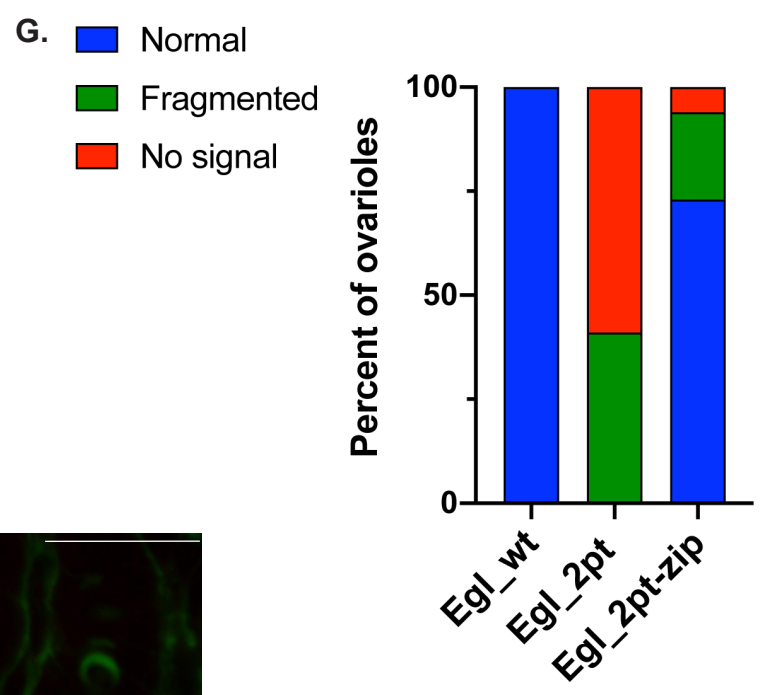

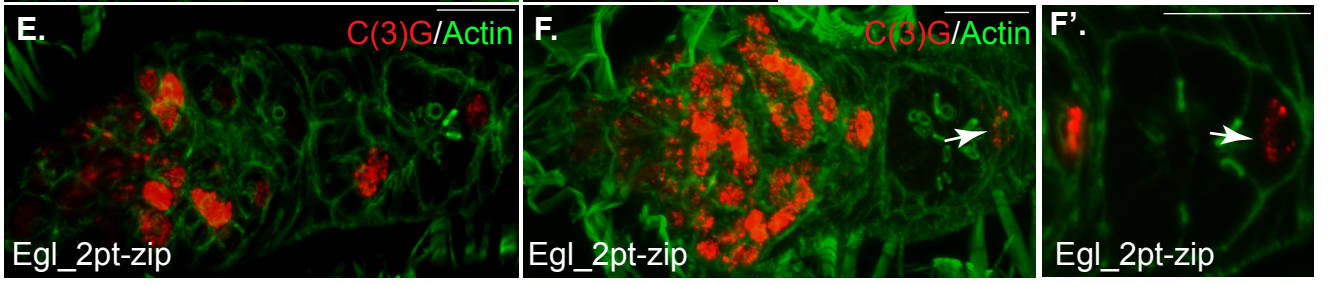

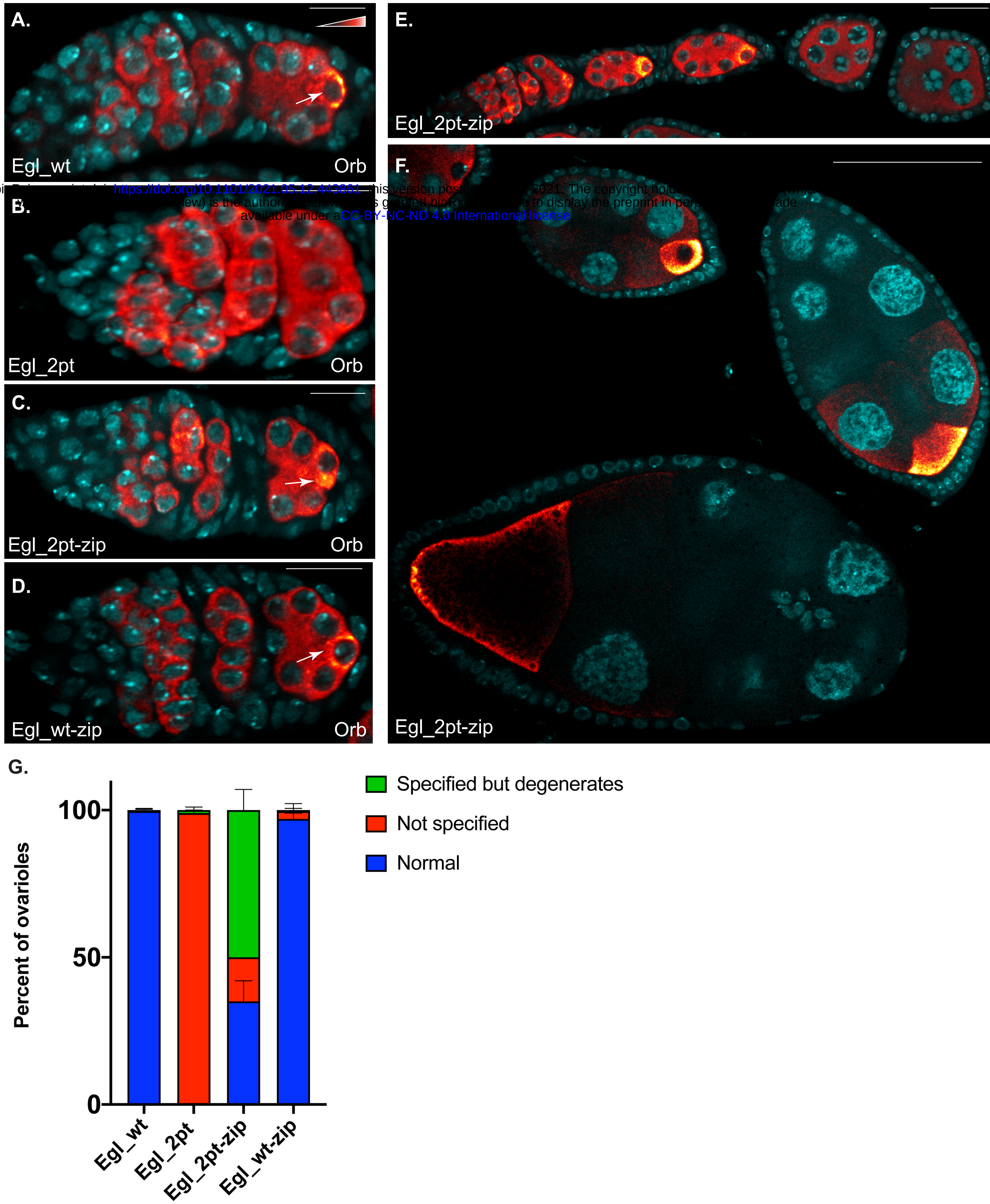

Figure 3

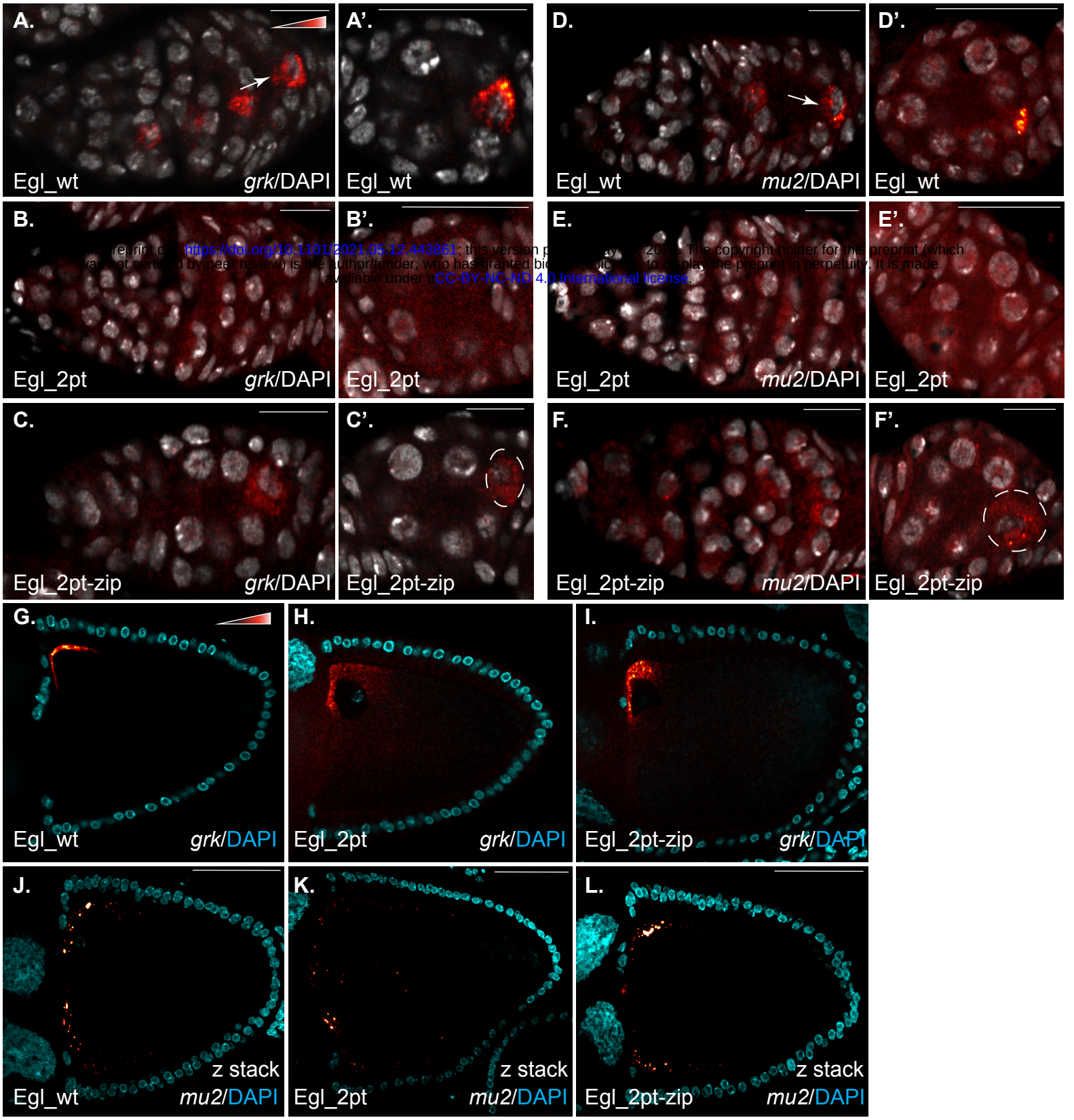

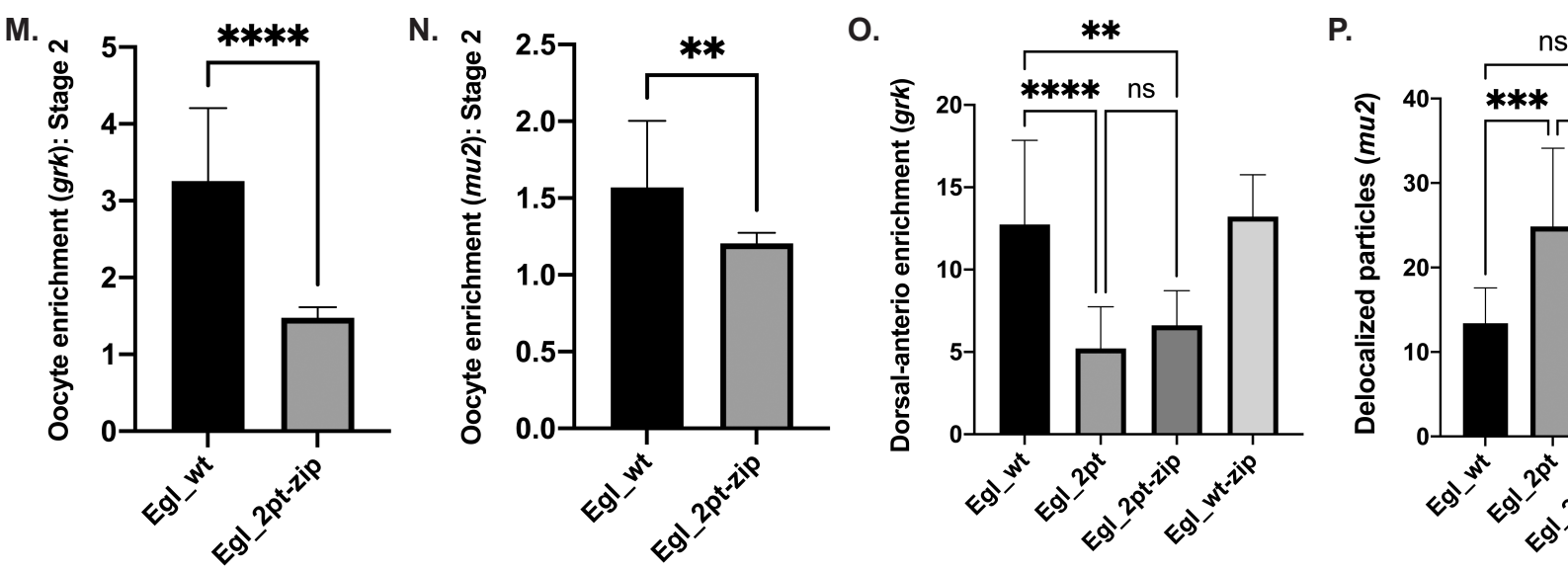

Figure 4

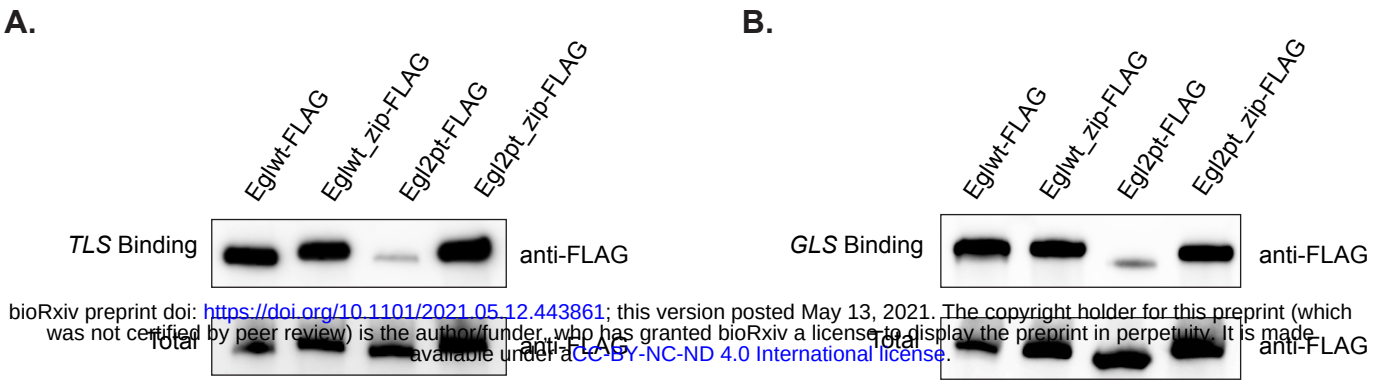

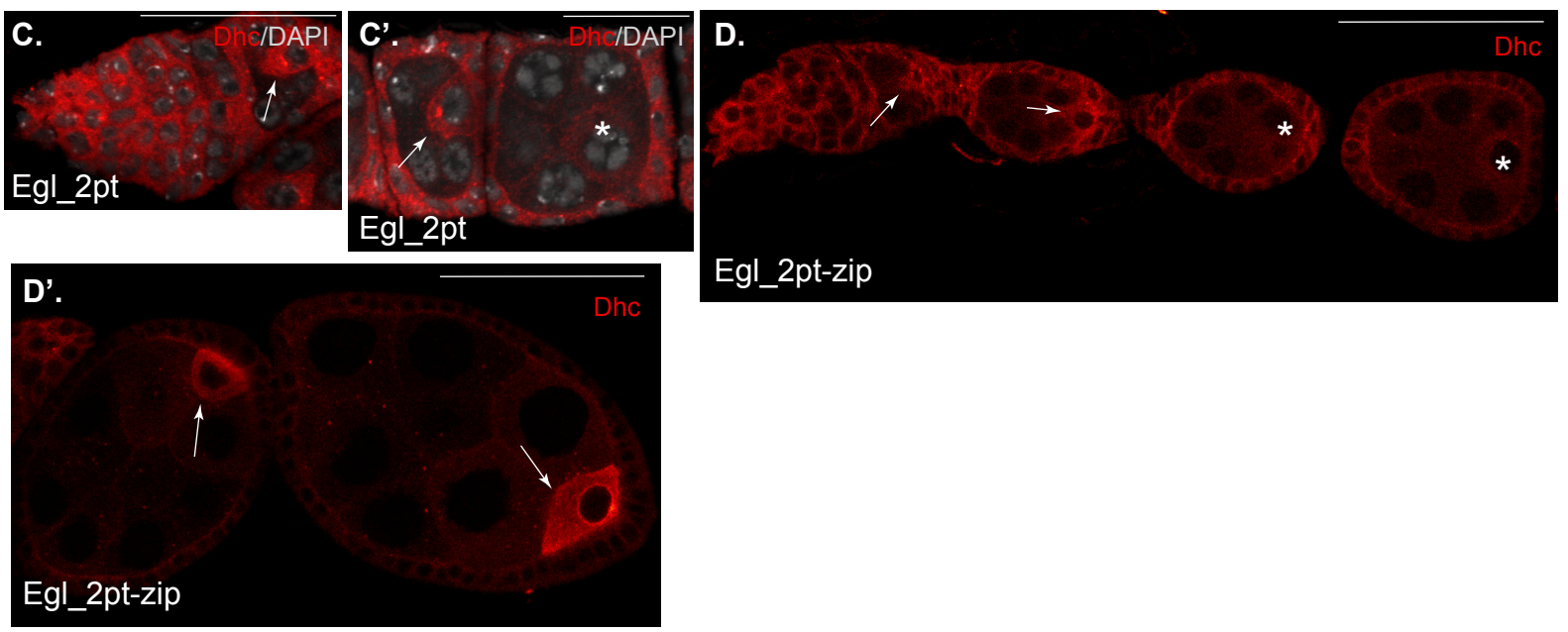

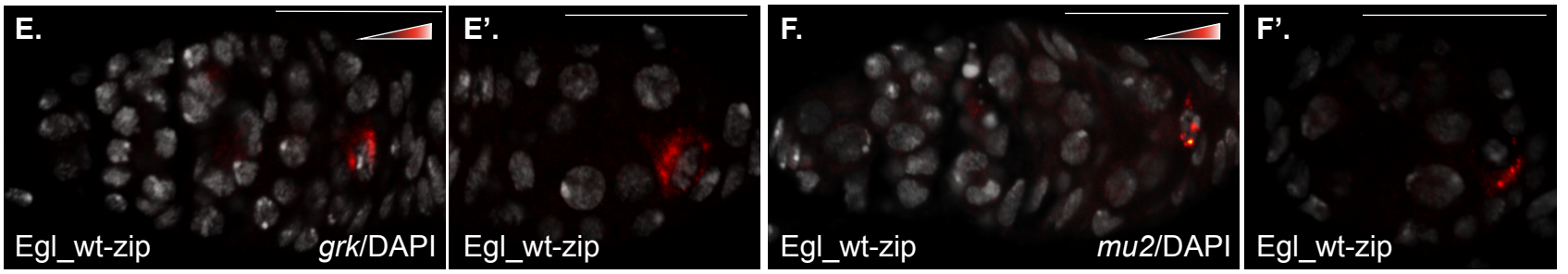

Supplemental Figure1

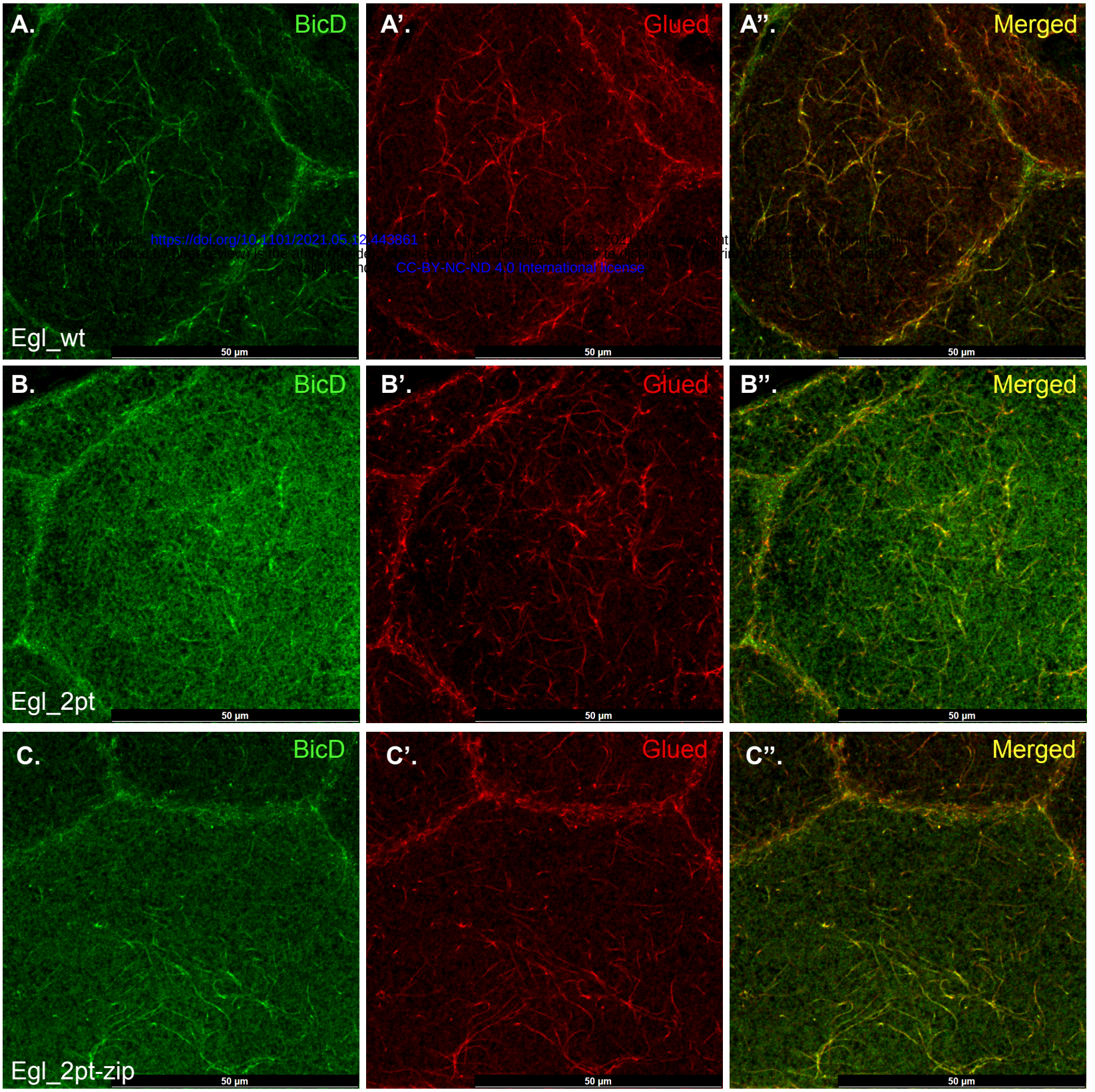

Supplemental Figure2